Rheol Acta (2010) 49:1219–1225
DOI 10.1007/s00397-010-0467-4

RAPID COMMUNICATION

Buckling instabilities in dilute polymer solution elastic strands

Simon J. Haward

Received: 8 January 2010 / Revised: 16 April 2010 / Accepted: 15 May 2010 / Published online: 6 June 2010

Abstract A microfluidic oscillatory cross-slot flow is used to visualize birefringent strands in dilute polystyrene solutions with high temporal resolution, focusing specifically on reversals in the flow direction. Due to polymer conformation hysteresis, the elastic strands are slow to relax and demonstrate a compressive modulus, resulting in a "buckling instability." An elastic loop of birefringence forms in an exit channel of the cross, seeding the development of a new birefringent strand in the perpendicular direction. These observations have major relevance to cyclic flows of polymer solutions (e.g., porous media flows where stagnation points are present) and for finitely extensible nonlinear elastic dumbbell modeling of such flows.

Keywords Polymer solution · Extensional flow · Stagnation point · Birefringence · Cyclic flow

Introduction

Extensional components arise in virtually all real fluid flows, in particular contraction/expansion flows, bifurcations, flow around obstacles, and stagnation points (Pipe and McKinley 2009). Many important industrial processes including porous media flow, which is relevant to enhanced oil recovery, involve the passage of complex polymeric fluids through exactly these kinds of geometries (Haward and Odell 2003; Odell and Haward 2006), so the importance of understanding the response of polymer solutions to extensional flows is clear.

In 1974, theoretical considerations showed that an equilibrium nonfree-draining coiled polymer molecule could extend and align in an extensional flow field provided the strain rate ($\dot{\varepsilon}$) exceeded the relaxation rate ($1/\tau_{c-s}$) of the polymer where τ_{c-s} is the characteristic stretching time, so that the dimensionless Deborah number, $De = \dot{\varepsilon}\tau_{c-s} >\sim 1$ (De Gennes 1974; Hinch 1974). As the polymer oriented and uncoiled in the flow, increasing frictional hydrodynamic interactions between the polymer and solvent meant that the uncoiling became a critical and run-away process in which the polymer molecule could become fully stretched. The increased segment–solvent interactions also meant that the polymer relaxation time would effectively increase when the polymer stretched, resulting in coil–stretch–coil hysteresis with strain rate. Additionally, the stretched polymers would cause a huge increase in the extensional viscosity.

The cross-slot is a stagnation point extensional flow device that has been used to test these predictions over three decades of work (e.g., Scrivener et al. 1979; Perkins et al. 1997; Arratia et al. 2006). A stagnation point is a singularity in a flow field where the flow velocity is zero but the strain rate, $\dot{\varepsilon}$, can be large. Hence, polymer molecules that follow streamlines through the stagnation point become trapped in the velocity gradient for, in principle, infinite time and can accumulate significant strain (e.g., Miles and Keller 1980; Perkins et al. 1997; Smith and Chu 1998). Birefringence studies with dilute solutions of monodisperse polymers in theta solvents (atactic polystyrene [aPS] in decalin) have

S. J. Haward (✉)
H.H. Wills Physics Department, University of Bristol,
Tyndall Avenue, Bristol, BS8 1TL, UK
e-mail: s.j.haward@bristol.ac.uk

shown that molecules stretch at a critical strain rate, $\dot{\varepsilon}_c$, indicating the characteristic stretching time $\tau_{c-s} = 1/\dot{\varepsilon}_c$ (Carrington and Odell 1996; Carrington et al. 1997a, b). Even at the highest dilutions, stretched polymers at the stagnation point are observed to form birefringent strands that extend along the exit channels of the cross-slot resulting in large increases in the pressure, indicating the predicted extensional viscosity increase (Odell and Carrington 2006). Coil–stretch relaxation time hysteresis has also been observed experimentally in the cross-slots, using fluorescently labeled DNA molecules (Schroeder et al. 2003), and by following the relaxation of flow-induced birefringence in polystyrene solutions after the cessation of flow (Haward et al. 2010).

Birefringent strands indicative of high degrees of macromolecular strain have also been observed in the flow of polymer solutions around spheres (Haward and Odell 2004) and in oscillatory contraction/expansion geometries (Cressely and Hocquart 1981). Birefringence has been measured to increase over successive passages through cylinder arrays and contraction/expansion geometries (Dyakonova et al. 1996). It is widely believed that stretching of macromolecules is responsible for the large increase in flow resistance observed in porous media flow of polymer solutions (e.g., Marshall and Metzner 1967; Haas and Durst 1982).

Modeling studies with finitely extensible nonlinear elastic (FENE) dumbbells in cross-slot flows show much better agreement with experimental observations when conformation-dependent hydrodynamic interactions are included (Remmelgas et al. 1999), consistent with theories of De Gennes and Hinch. However, such models cannot predict the accumulation of macromolecular strain observed experimentally in symmetric periodic flows (Nollert and Olbricht 1985; Saphiannikova et al. 2000). In this case, the strain accumulated by the dumbbell on passing through a contraction is entirely lost during passage through a subsequent symmetric expansion. One possible explanation for the discrepancy between theory and experiment is a breaking of symmetry in the real flow due to inertial effects. It has been shown that FENE dumbbells could accumulate strain under such circumstances (Dyakonova et al. 1996).

This letter reports the use of a recently developed oscillatory microfluidic cross-slot device called the extensional flow oscillatory rheometer (EFOR; Odell and Carrington 2006) to study dilute polystyrene solutions. Some highly unusual and unexpected birefringent structures are reported, which provide valuable insight into the nature of stretched polymer strands and also have important implications for polymer stretching/relaxation processes in cyclic extensional flows and hence for dumbbell modeling of such flows.

Experimental

The EFOR generates a stagnation point extensional flow using a piezoelectric micropump on each arm of a cross-slot (see Fig. 1). The micropumps are driven by applying oscillating triangular voltage profiles of amplitude V and period T across them. The stagnation point remains at the center of the cross, but the oscillation means that fluid is pumped into one pair of opposite channels and out of the second pair for a time $T/2$, before the flow is reversed for a time $T/2$ and the cycle repeats. Hence, a given fluid element experiences a cyclic flow characterized by repeated passage through the cross-slot. The experiment is highly relevant to a porous media flow in which a fluid element may pass through, or near to, a succession of stagnation points.

The micropumps provide a linear displacement of fluid and hence a constant volume flow rate $Q(\propto V/T)$ through each channel of the slot. The strain rate is given by:

$$\dot{\varepsilon} = \frac{2Q}{d^2 t}. \tag{1}$$

The slots used in this study have a channel width of $d = 200$ μm and a depth of $t = 1$ mm, giving an aspect ratio of 5:1. The total length of each channel is $L = 1.2$ mm.

Birefringence in the cross-slot was visualized essentially using the optical set-up illustrated schematically in Fig. 1. The polarizer and analyzer were initially crossed at ±45° to the axes of flow to extinguish the light from the temperature-stabilized, spatially filtered 660-nm, 50-mW fiber-coupled diode laser from Oz-

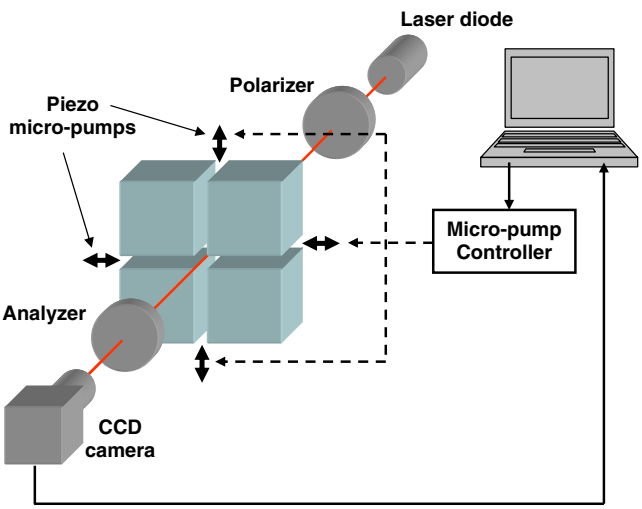

Fig. 1 Schematic of oscillatory cross-slot flow system, including optical line and piezo micropump control

Optics. A λ/4 plate was inserted to compensate for residual birefringence in the optical line, before the polarizer was slightly uncrossed (<3°) to allow a background signal through in order to increase the signal to noise ratio for flow-induced birefringence (Riddiford and Jerrard 1970). A cylindrical lens was inserted horizontally to spread the laser light along the horizontal inlet/outlet arms of the cross. The CCD camera was a deeply cooled (−80°C), low-noise, high-quantum efficiency, 14-bit, megapixel model from Andor Technology. Using the camera driver software (Image Pro Plus), a "letter box"-shaped region of interest was selected around the horizontal inlet/outlet channel and the pixels were binned in order to increase the frame capture rate to ~360 frames per second.

The polymer solutions were 0.03 wt.% solutions of aPS in dioctyl phthalate (DOP). The molecular weights were $M_p = 6.9 \times 10^6$ and 10.2×10^6 Da, both with low polydispersity index $M_w/M_n \sim 1.15$. DOP is a fairly viscous ($\eta = 0.046$ Pa s) theta solvent for aPS at close to room temperature. The viscous DOP solvent and the microscale of the flow geometry mean inertial effects are negligible; the Reynolds number, *Re*, is <0.5 in all the experiments. The overlap concentration for this system is $c^* \sim 0.3$ wt.%, so the polymer solutions are well into the dilute regime.

Values for the mean characteristic stretching times, τ_{c-s}, for the polymer samples were found from the inverse of the critical strain rate, $\dot{\varepsilon}_c$, required to stretch the polymer in a cross-slot, as determined from birefringence measurements (Haward et al. 2010). The coil–stretch relaxation time was found to depend on molecular weight according to the prediction of Zimm (1956), i.e., $\tau_{c-s} \propto M_w^{1.5}$; therefore, there is a spectrum of relaxation times for each polymer sample that corresponds to the narrow molecular weight distribution. Values were found of $\tau_{c-s} \sim 4$ ms and $\tau_{c-s} \sim 7$ ms corresponding to the peak molecular weights of the 6.9− and 10.2-MDa samples, respectively. Haward et al. also measured the decay of birefringence in the cross-slot following the cessation of flow and used this information to find characteristic times for the relaxation of the polymer molecules from stretch, τ_{s-c}. These were found to be ~130 and ~250 ms for the 6.9− and 10.2-MDa samples, respectively. Hence, the relaxation time increases by a factor of ~35 when the aPS molecule undergoes the coil–stretch transition. This increase in relaxation time when polymer molecules stretch from a highly coiled state in a theta solvent is consistent with the expectations of De Gennes and Hinch. This is due to the transition from nonfree-draining (coiled) to free-draining (stretched) conditions and the corresponding increase in hydrodynamic interactions with the solvent.

Results and discussion

Figure 2 shows a sequence of images illustrating what happens to a birefringent strand in the cross-slot when the flow undergoes a reversal after half a pump cycle period, *T*/2. Figure 2a shows the existing horizontal birefringent strand extending from the stagnation point along the exit channel of the cross, immediately before the pumps reverse direction (the position of the stagnation point is indicated by the white "x" superimposed on Fig. 2d). After the flow has reversed, the birefringent strand is initially buckled upwards toward the top exit channel (Fig. 2b, c) before strands from the left- and right-hand channels are seen disappearing into the top channel (Fig. 2d, e). A vertical birefringent strand becomes visible in Fig. 2e, f. (Due to the method of birefringence detection, vertical orientation of polymer chains results in a dark signal, whereas horizontal orientation produces a bright signal. For example, in Fig. 2e, the bright horizontal strand becomes dark where it turns the 90° corner into the top exit channel.) Interestingly, even after the new vertically oriented birefringent strand has formed (Fig. 2f), the original bright horizontal strand is still faintly visible.

Figure 3 illustrates what happens when the flow undergoes a second reversal. In Fig. 3a, the dark vertical strand has already buckled to the left of the stagnation point and has been displaced a short distance into the new horizontal exit channel. In Fig. 3b, c, it becomes apparent that the vertical birefringent strand is being dragged from the top and bottom channels, forming a birefringent loop in the exit channel. The trailing ends of the loop then appear to play a role in "nucleating" the formation of the new horizontal birefringent strand

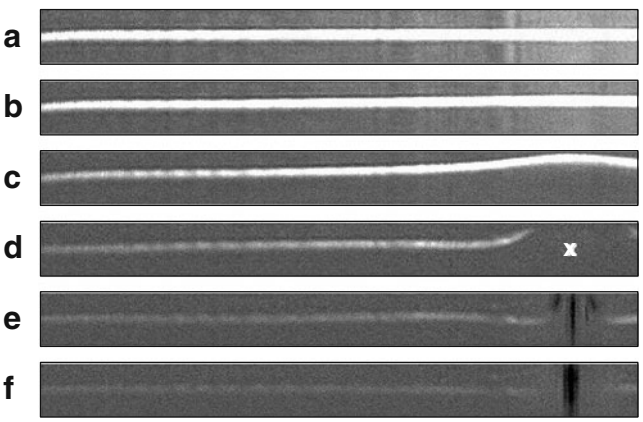

Fig. 2 Reversal of flow in the oscillatory cross-slot. Time since pump reversal: *a* 0.0 s, *b* 17 ms, *c* 36 ms, *d* 56 ms, *e* 76 ms, *f* 95 ms. 0.03% 10.2-MDa aPS in DOP, $\dot{\varepsilon} = 410\ s^{-1}$, $De \sim 2.9$. The *white x* in *d* marks the stagnation point

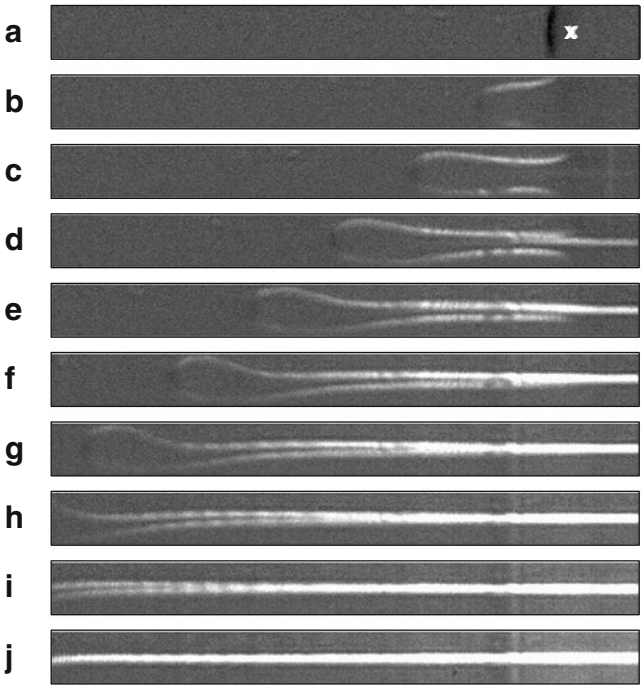

Fig. 3 Reversal of flow in the oscillatory cross-slot. Time since pump reversal: *a* 42 ms, *b* 56 ms, *c* 64 ms, *d* 73 ms, *e* 81 ms, *f* 90 ms, *g* 98 ms, *h* 106 ms, *i* 118 ms, *j* 146 ms. 0.03% 10.2-MDa aPS in DOP, $\dot{\varepsilon} = 410\ s^{-1}$, $De \sim 2.9$. The *white x* in *a* marks the stagnation point

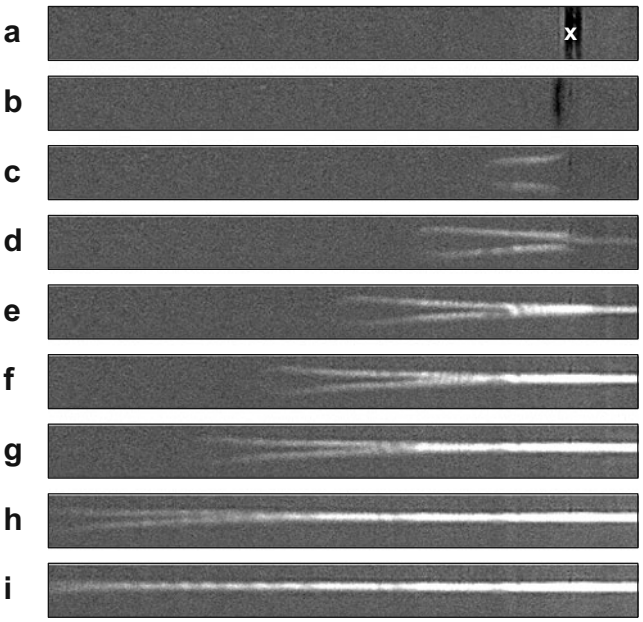

Fig. 4 Development of a birefringent strand following reversal of flow in the oscillatory cross-slot. Time since pump reversal: *a* 0 ms, *b* 42 ms, *c* 70 ms, *d* 84 ms, *e* 98 ms, *f* 112 ms, *g* 126 ms, *h* 54 ms, *i* 182 ms. 0.03% 10.2-MDa aPS in DOP, $\dot{\varepsilon} = 205\ s^{-1}$, $De \sim 1.5$. The *white x* in *a* marks the stagnation point

(Fig. 3d–f). The birefringent loop remains attached to the newly forming horizontal strand as it flows away from the stagnation point and extends along the exit channel (Fig. 3f–i). Finally, in Fig. 3j, the formation of the new birefringent strand is complete, a pump cycle is complete, and the flow has returned to the original state seen in Fig. 2a.

Very similar observations have been made over a range of strain rates, as shown in Figs. 4 and 5, for the flow of the 0.03-wt.% 10.2-MDa aPS solution at $\dot{\varepsilon} = 205\ s^{-1}$ and $\dot{\varepsilon} = 920\ s^{-1}$, respectively. Additionally, Fig. 6 shows the same phenomena with the 0.03-wt.% 6.9-MDa aPS solution flowing at $\dot{\varepsilon} = 410\ s^{-1}$.

There are many interesting points to note about the birefringence observations in Figs. 2–6. The fact that the horizontal birefringent strand remains existent after a flow reversal and is deflected toward the upper exit channel (Fig. 2b, c) indicates that the strand has a degree of resistance to compression, i.e., a compressive modulus. Prior to these experiments, the expectation was that, on reversing the stress on the birefringent strand, the macromolecular strain would relax extremely quickly and the birefringence would vanish. In fact, the strand remains quite stable and behaves similar to a flexible sheet of solid material under a compressive load; the sheet has to buckle in one of two possible directions perpendicular to the load. Presumably, any small perturbation or asymmetry in the flow will determine whether the strand buckles toward the upper or lower exit channel. It should be noted that the EFOR has an extremely symmetric flow; pumped

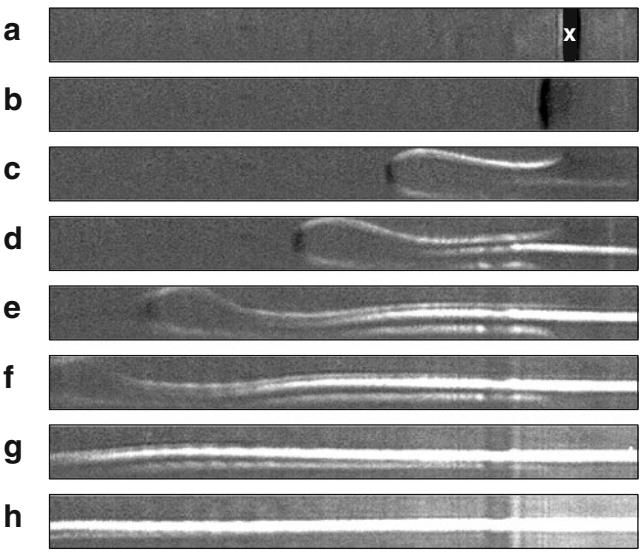

Fig. 5 Development of a birefringent strand following reversal of flow in the oscillatory cross-slot. Time since pump reversal: *a* 0 ms, *b* 28 ms, *c* 42 ms, *d* 48 ms, *e* 56 ms, *f* 62 ms, *g* 70 ms, *h* 84 ms. 0.03% 10.2-MDa aPS in DOP, $\dot{\varepsilon} = 920\ s^{-1}$, $De \sim 6.5$. The *white x* in *a* marks the stagnation point

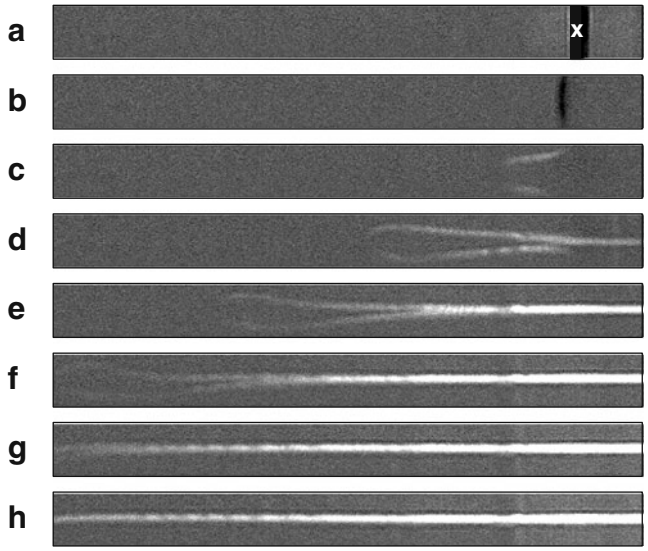

Fig. 6 Development of a birefringent strand following reversal of flow in the oscillatory cross-slot. Time since pump reversal: *a* 0 ms, *b* 42 ms, *c* 56 ms, *d* 70 ms, *e* 84 ms, *f* 98 ms, *g* 112 ms, *h* 126 ms. 0.03% 6.9-MDa aPS in DOP, $\dot{\varepsilon} = 410\ s^{-1}$, $De \sim 1.6$. The *white x* in *a* marks the stagnation point

volumes vary by not more than 2% in each channel of the cross and the cross itself is made to extremely high tolerance by wire electrical discharge machining. The symmetrical nature of the flow is demonstrated by Fig. 7, which shows a vector map of the steady

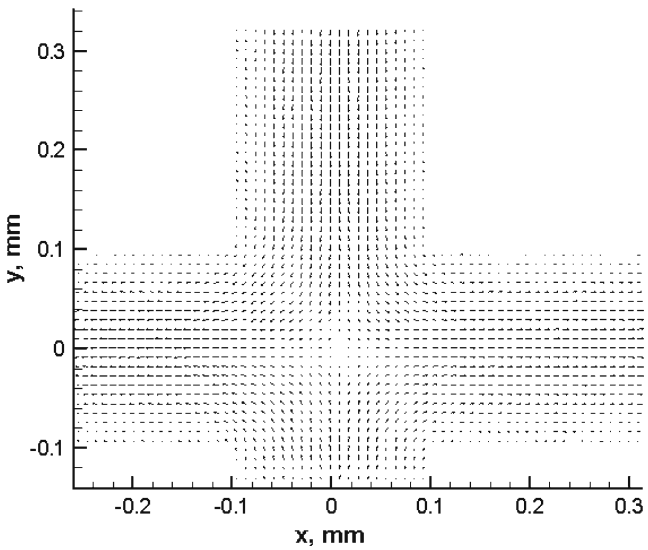

Fig. 7 Newtonian flow field for DOP in the cross-slot, demonstrating the highly symmetric nature of the flow about the stagnation point at the center of the cross. The image represents a 13.6-μm thick slice through the midplane of the cross-slot. The Reynolds number is ~0.5

Newtonian flow field obtained by microparticle image velocimetry.

Preliminary flow simulations using the linear Phan-Thien–Tanner model indicate that birefringent strands will buckle at high De ($De \sim 70$) in an initially completely symmetric flow field, with the direction of buckling depending on the choice of model parameters (Omowunmi 2010, personal communication). Of course, the buckling itself subsequently breaks the symmetry of the flow field. Experimentally, the birefringent strand was almost always observed to buckle toward the top exit channel (as in Fig. 2) or toward the left exit channel (as in Figs. 3–6), indicating that there was probably some small degree of asymmetry introduced by the geometry or the flow which caused the strand to favor buckling in these directions. Clearly, perfect flow symmetry is impossible to achieve in an experimental situation; however, it is almost inconceivable that any real flow, such as around obstacles or through porous media, will be as symmetric as the flow in the EFOR.

The resistance to compression demonstrated by the elastic strand is likely to be due to the increased relaxation time of the polymer in the stretched state. As described above, Haward et al. (2010) have shown that the relaxation time for aPS in DOP increases by a factor of $\tau_{s-c}/\tau_{c-s} \sim 35$ following the coil–stretch transition. Hence, when the polymer becomes stretched, the deformation rate becomes hugely greater than the relaxation rate of the polymer and the polymer cannot relax on the time scale of the flow. What may be a fairly moderate-sounding Deborah number of $De = 2.9$ for coiled molecules (as in Figs. 2 and 3) could be considered as $De \sim 100$ for the stretched molecules in the birefringent elastic strand. Consequently, the strand behaves essentially as an elastic solid.

A clear consequence of the resulting buckling is that the return path of the stretched birefringent material is not through the stagnation point. In fact, Fig. 2d shows particularly clearly that the stretched material can pass far from the stagnation point on its return journey through the cross-slot. The implication of this is clear for a cyclic flow: in order for macromolecular strain and relaxation to be equal and opposite over a cycle, a fluid element must flow to-and-fro along the same stream line. If a fluid element flows though the stagnation point, a large strain can be accumulated. By following a different streamline and avoiding the stagnation point on the return journey, symmetry is broken and the accumulated strain is not completely relaxed.

The effect of the loop of birefringence that forms in the new exit channel after a flow reversal is to present prestretched material close to the stagnation

point as the trailing ends of the loop are pulled into the exit channel (e.g., Fig. 3c–e). This appears to initiate a high degree of stretching at the stagnation point, from which the new birefringent strand forms. Implications for cyclic flows, such as porous media where stagnation points are present, are again clear. Stretched polymer strands are clearly long-lived and resilient entities and, where multiple stagnation points are present, prestretched material coming from one stagnation point may be expected to facilitate further stretching at downstream stagnation points, resulting in a high degree of viscosity and pressure drop enhancement. It should be noted that all the effects described have also been observed in solutions at concentrations as low as 0.005 wt.% ($c^*/c \sim 100$).

There is a strong parallel between the present observations and those of Haward and Odell (2004) for flow around two aligned spheres. The birefringent strands originating from the trailing stagnation point of the first sphere were observed not to approach the leading stagnation point of the second sphere, but rather to buckle and flow around the second sphere, remaining intact. However, rather than seeding an intense birefringent strand behind the second sphere, the elastic strands from the first sphere effectively screened the trailing stagnation point of the second sphere from the flow field, resulting in a lower birefringence there. Although this seems to be contradictory to the current observations, it is likely to be explained by the divergent flow around the sphere.

An interesting parallel experiment could be devised in which the outlet from one cross-slot was fed directly into a second cross-slot. This would allow the effect of a downstream stagnation point on prestretched material to be observed under steady-state flow conditions. Future studies could also investigate the influence of solvent viscosity and solvent quality on the dynamics of the elastic strands. Using a good solvent, as opposed to the theta solvent used here, would result in more free-draining random coils and would, therefore, be expected to reduce the ratio of τ_{s-c}/τ_{c-s}.

Conclusions

In conclusion, high-speed video imaging of birefringent elastic strands in the EFOR has given new insights into the properties and transient behavior of the strands. Unexpected effects, i.e., the buckling of the strand after a flow reversal and the seeding of a new strand by the remnants of the old one, have been observed even at very high dilutions. This provides an explanation for the large non-Newtonian effects observed in complex cyclic flows of dilute polymer solutions, such as through porous media. The symmetry breaking of the flow on its return through the cross gives a possible explanation for cumulative polymer stretching in apparently symmetrical periodic flows and hence for why most FENE dumbbell simulations do not model polymer stretching in such oscillatory flows well.

Acknowledgements I gratefully acknowledge the Engineering and Physical Sciences Research Council (EPSRC), UK, for the funding. I am indebted to Dr. JA Odell (Bristol University) for the helpful discussions and to Dr. Z. Li (Manchester University) for helping with the microparticle image velocimetry.

References

Arratia PE, Thomas CC, Diorio J, Gollub JP (2006) Elastic instabilities of polymer solutions in cross channel flow. Phys Rev Lett 96:144502

Carrington SP, Odell JA (1996) How do polymers stretch in stagnation point extensional flow fields? J Non-Newton Fluid Mech 67:269–283

Carrington SP, Tatham JP, Odell JA, Saez AE (1997a) Macromolecular dynamics in extensional flows: 1. Birefringence and viscometry. Polymer 38:4151–4164

Carrington SP, Tatham JP, Odell JA, Saez AE (1997b) Macromolecular dynamics in extensional flows: 2. The evolution of molecular strain. Polymer 38:4595–4607

Cressely R, Hocquart R (1981) Extension and relaxation of high macromolecules in oscillatory elongational flow using flow birefringence. Polymer Prepr 22:120–121

De Gennes PG (1974) Coil–stretch transition of dilute flexible polymers under ultrahigh velocity gradients. J Chem Phys 60:5030–5042

Dyakonova NE, Odell JA, Brestkin YV, Lyulin AV, Saez AE (1996) Macromolecular strain in periodic models of porous media flows. J Non-Newton Fluid Mech 67:285–310

Haas R, Durst F (1982) Viscoelastic flow of dilute polymer solutions in regularly packed beds. Rheol Acta 21:566–571

Haward SJ, Odell JA (2003) Viscosity enhancement in non-Newtonian flow of dilute polymer solutions through crystallographic porous media. Rheol Acta 42:516–526

Haward SJ, Odell JA (2004) Molecular orientation in non-Newtonian flow of dilute polymer solutions around spheres. Rheol Acta 43:350–363

Haward SJ, Odell JA, Li Z, Yuan X-F (2010) Extensional rheology of dilute polymer solutions in oscillatory cross-slot flow: the transient behaviour of birefringent strands. Rheol Acta. doi:10.1007/s00397-009-0420-6

Hinch EJ (1974) Mechanical models of dilute polymer solutions for strong flows with large polymer deformations. Polymeres et Lubrification, Colloques Internationaux du CNRS 233:241–247

Marshall RJ, Metzner AB (1967) Flow of viscoelastic fluids through porous media. Ind Eng Chem Fundam 6:393–400

Miles MJ, Keller A (1980) Conformational relaxation time in polymer solutions by elongational flow experiments 2. Preliminaries of further developments: chain retraction; iden-

tification of molecular weight fractions in a mixture. Polymer 21:1295–1298
Nollert MU, Olbricht WL (1985) Macromolecular deformation in periodic extensional flows. Rheol Acta 24:3–14
Odell JA, Carrington SP (2006) Extensional flow oscillatory rheometry. J Non-Newton Fluid Mech 137:110–120
Odell JA, Haward SJ (2006) Viscosity enhancement in non-Newtonian flow of dilute aqueous polymer solutions through crystallographic and random porous media. Rheol Acta 45: 853–863
Perkins TT, Smith DE, Chu S (1997) Single polymer dynamics in an elongational flow. Science 276:2016–2021
Pipe CJ, McKinley GH (2009) Microfluidic rheometry. Mech Res Comm 36:110–120
Remmelgas J, Singh P, Leal LG (1999) Computational studies of nonlinear elastic dumbbell models of Boger fluids in a cross-slot flow. J Non-Newton Fluid Mech 88:31–61
Riddiford CL, Jerrard HG (1970) Limitations on the measurement of relaxation times using a pulsed Kerr effect method. J Phys D Appl Phys 3:1314–1321
Saphiannikova MG, Darinskii AA, Dyakonova NE (2000) Computer simulation of dilute polymer solutions in transient elongational flows. Macromol Theory Simul 9:270–280
Schroeder CM, Babcock HP, Shaqfeh ESG, Chu S (2003) Observation of polymer conformation hysteresis in extensional flow. Science 301:1515–1519
Scrivener O, Berner C, Cressely R, Hocquart R, Sellin R, Vlachos NS (1979) Dynamical behaviour of drag-reducing polymer solutions. J Non-Newton Fluid Mech 5:475–495
Smith DE, Chu S (1998) Response of flexible polymers to sudden elongational flow. Science 281:1335–1340
Zimm BH (1956) Dynamics of polymer molecules in dilute solution: viscoelasticity, flow birefringence and dielectric loss. J Chem Phys 24:269–278